

Cite this: *CrystEngComm*, 2011, **13**, 4909

www.rsc.org/crystengcomm

PAPER

Iron(II) thio- and selenocyanate coordination networks containing 3,3'-bipyridine†

Christopher J. Adams,^{*a} Mairi F. Haddow,^a David J. Harding,^b Thomas J. Podesta^a and Rachel E. Waddington^a

Received 23rd March 2011, Accepted 31st May 2011

DOI: 10.1039/c1ce05352c

A number of different compounds have been synthesised by reaction of solutions containing $\text{Fe}(\text{NCE})_2$ ($\text{E} = \text{S}, \text{Se}$) with solutions containing 3,3'-bipyridine. When the solvent used is methanol, the products are the monomeric compounds *trans*- $\{\text{Fe}(\text{NCS})_2(3,3'\text{-bipy})_2(\text{MeOH})_2\}$ **1** or *trans*- $\{\text{Fe}(\text{NCSe})_2(3,3'\text{-bipy})_2(\text{MeOH})_2\}$ **2**, but when acetonitrile is used the layered coordination network $\{\text{Fe}(\text{NCS})_2(3,3'\text{-bipy})_2\}$ **3** or doubly interpenetrated coordination network $\{\text{Fe}(\text{NCSe})_2(3,3'\text{-bipy})_2\}$ **4** is formed instead. Using methanol to dissolve the $\text{Fe}(\text{NCE})_2$ and CHX_3 ($\text{X} = \text{Cl}, \text{Br}$) to dissolve the 3,3'-bipyridine yields solvated coordination networks of stoichiometry $\{\text{Fe}(\text{NCE})_2(3,3'\text{-bipy})_2\} \cdot 2\text{CHX}_3$. The crystal structures of all of these compounds except **4** are presented.

Introduction

Whereas 4,4'-bipyridine is somewhat ubiquitous in the field of coordination networks and polymers,¹ its cousin 3,3'-bipyridine (3,3'-bipy) is virtually absent. This is probably due to two major factors: firstly, 4,4'-bipyridine is commercially available but 3,3'-bipyridine is not, and secondly, 4,4'-bipyridine is an easy to handle crystalline solid but 3,3'-bipyridine is hygroscopic and tends to become an oil unless completely dry.² That 3,3'-bipyridine containing coordination networks and polymers do exist is largely due to the efforts of LaDuca and co-workers, who have reported the preparation of several different types which incorporate a variety of metals and co-ligands.^{3–11}

Of interest to us was the reported preparation of two different networks with stoichiometry $\{\text{M}(\text{NCS})_2(3,3'\text{-bipy})_2\}$ ($\text{M} = \text{Ni}, \text{Co}$).¹¹ This implied that it might also be possible to synthesise $\{\text{Fe}(\text{NCS})_2(3,3'\text{-bipy})_2\}$, which would have a ligand set ($2 \times$ thiocyanate anions and $4 \times$ pyridyl rings) at the iron that might allow it to exhibit spin-crossover (SCO) behaviour; several coordination networks with an iron atom in this coordination environment are known to show SCO.^{12–15} Particularly interesting was the fact that $\{\text{Ni}(\text{NCS})_2(3,3'\text{-bipy})_2\}$ forms a doubly interpenetrated adamantoid network of 6⁶ topology;¹¹ as interpenetrated iron-containing networks often show guest-modulated SCO behaviour,^{12,13,15} we were keen to establish whether this particular network could also be synthesised with iron, and we report below the results we obtained in attempting this. In

contrast, $\{\text{Co}(\text{NCS})_2(3,3'\text{-bipy})_2\}$ forms a non-interpenetrated layered structure composed of parallel (4,4)-grids, similar to the structures of several $\{\text{M}(\text{NCS})_2(4,4'\text{-bipy})_2\}$ networks.¹⁶ However, whereas the 4,4'-bipyridine networks are more-or-less square grids, with metal atoms as the nodes and the linear bidentate ligand as the edges, the structure of $\{\text{Co}(\text{NCS})_2(3,3'\text{-bipy})_2\}$ is rather distorted due to the non-linear nature of the bridging ligand.¹¹

Results and discussion

Synthesis of 3,3'-bipyridine

Previous approaches to the synthesis of this ligand include a nickel(0) mediated coupling of 3-bromopyridine,² or a Stille coupling of 3-trimethylstannylpyridine (which is complicated by the synthesis of this reagent).¹⁰ We have used a different approach, using a palladium-catalysed homocoupling of 3-bromopyridine,¹⁷ which gives a clean reaction requiring a straightforward workup. As previously reported, the product is a hygroscopic oil which solidifies after several days drying over P_2O_5 .²

Synthesis of monomeric compounds

We have previously successfully prepared $\{\text{M}(\text{NCS})_2(4,4'\text{-bipy})_2\}$ networks by slow diffusion of a solution of 4,4'-bipyridine into a methanolic solution of $\text{Fe}(\text{NCS})_2$ (prepared *in situ* from FeSO_4 and KNCS),¹⁶ in which case using different solvents to dissolve the bipyridine allowed preparation of the same basic network incorporating different solvents of crystallisation. However, adopting the same approach with 3,3'-bipyridine as the ligand often yielded not the target coordination network $\{\text{Fe}(\text{NCS})_2(3,3'\text{-bipy})_2\}$, but crystals of the unanticipated compound *trans*- $\{\text{Fe}(\text{NCS})_2(3,3'\text{-bipy})_2(\text{MeOH})_2\}$ **1**. The 3,3'-bipyridine

^aSchool of Chemistry, University of Bristol, Bristol, BS8 1TS, U.K. E-mail: chcja@bris.ac.uk

^bMolecular Technology Research Unit, Department of Chemistry, Walailak University, Thasala, Nakhon Si, Thammarat, 80161, Thailand

† Electronic supplementary information (ESI) available. CCDC reference numbers 818774–818781. For ESI and crystallographic data in CIF or other electronic format see DOI: 10.1039/c1ce05352c

ligands in **1** are both monodentate, leading to a discrete molecular compound rather than a coordination polymer of any kind. There are, however, hydrogen bonds between the uncoordinated pyridyl nitrogen atom and the OH group of a methanol ligand attached to an adjacent metal centre, and because the 3,3'-bipyridine adopts a relatively planar conformation (the torsion angle between the pyridyl rings is about 16°) these hydrogen-bonds serve to link the molecules into a one-dimensional chain (Fig. 1). The overall structure is then comprised of parallel chains of this type, with no hydrogen bonds between chains. **1** may be readily synthesised in bulk by simply mixing methanolic solutions of 3,3'-bipyridine and iron thiocyanate.

Thermogravimetric analysis (see ESI) of **1** reveals that the methanol molecules may be eliminated by heating at above 125 °C. Removing the methanol from the crystal structure creates two vacant coordination sites which are in close proximity to the unbonded pyridyl ring, so it is easy to envisage how a topochemical solid-state chemical transformation might produce a one-dimensional coordination polymer of stoichiometry $\{\text{Fe}(\text{NCS})_2(3,3'\text{-bipy})_2\}$. However, such a compound is not known (for any metal), and the XRPD pattern (Fig. 2) of the product of this transformation shows that it is instead comprised largely of the two-dimensional $\{\text{Fe}(\text{NCS})_2(3,3'\text{-bipy})_2\}$ grid **3** (*vide infra*).

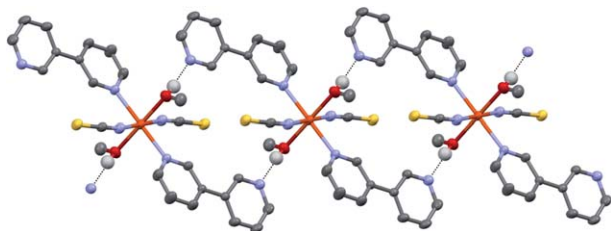


Fig. 1 Individual molecules of **1** are linked into 1-dimensional chains by OH...N hydrogen bonds. All hydrogen atoms except those involved in hydrogen bonding have been removed for clarity.

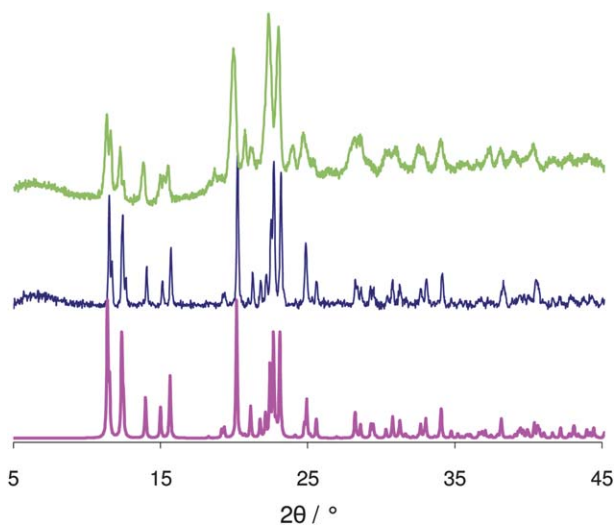


Fig. 2 Powder patterns for the two-dimensional $\{\text{Fe}(\text{NCS})_2(3,3'\text{-bipy})_2\}$ grid **3**: calculated from the crystal structure (pink), powder synthesised by dropwise addition in acetonitrile (blue), and by thermal decomposition of **1** at 150 °C under N_2 (green).

Table 1 Selected bond lengths (Å) and angles (°) for the structures of **1** and **2**

	1 (E = S)	2 (E = Se)
Fe–NCS	2.1244(12)	2.1203(12)
Fe–N _{bipy}	2.2693(11)	2.2699(11)
Fe–O	2.1201(11)	2.1118(11)
N–CE	1.1672(18)	1.1603(18)
NC–E	1.6298(13)	1.7851(13)
Fe–N–CE	158.29(11)	165.01(11)
Fe–O–Me	126.11(10)	126.57(10)
O(H) ... N	2.727	2.703
Fe–O(H) ... N	119.44	118.81

Replacing the thiocyanate ligands of **1** with selenocyanate gives analogous chemistry. Thus, mixing methanolic solutions of 3,3'-bipyridine and iron selenocyanate (prepared *in situ* from FeSO_4 and KNCSe) gives not the coordination network $\{\text{Fe}(\text{NCSe})_2(3,3'\text{-bipy})_2\}$ **4** (*vide infra*) but *trans*- $\{\text{Fe}(\text{NCSe})_2(3,3'\text{-bipy})_2(\text{MeOH})_2\}$ **2**, whose crystal structure we have also determined and which is isostructural with **1**. Thermal decomposition of **2** gives a phase **4** which appears to be isostructural with **3** (X-ray powder diffraction patterns are presented in the ESI), and which analyses correctly for two-dimensional $\{\text{Fe}(\text{NCSe})_2(3,3'\text{-bipy})_2\}$. Selected bond lengths and angles for **1** and **2** are given in Table 1, and crystallographic details for all compounds are presented in Table 2.

Synthesis of coordination networks

As reported above, mixing methanolic solutions of 3,3'-bipyridine and iron thiocyanate does not produce the coordination network $\{\text{Fe}(\text{NCS})_2(3,3'\text{-bipy})_2\}$ **3**. However, repeating the reaction in acetonitrile leads to clean formation of **3** as a microcrystalline solid, with better crystallinity and purity than the samples produced by heating **1**. Crystals of **3** were grown by dissolving both components of the crystallisation in acetonitrile and allowing them to diffuse together, and it is isostructural with the known cobalt-containing network.

Layered two-dimensional structures of this kind have been termed *Elastic Layer-structured Metal organic frameworkS* (*ELMS*) owing to the fact that they can act as hosts for gases or solvents by accommodating the guest between layers, increasing the inter-layer separation but keeping the layers essentially unchanged.¹⁸ We have recently discovered how such guests can alter the spin-crossover behaviour of the $\{\text{Fe}(\text{NCX})_2(4,4'\text{-bipy})_2\}$ two-dimensional network, and we hoped that this would also prove to be the case in the 3,3'-bipy system reported herein. To that end we grew crystals of **3** and of its selenocyanate analogue $\{\text{Fe}(\text{NCSe})_2(3,3'\text{-bipy})_2\}$ **4** from various combinations of solvent, with the aim of accommodating that solvent between layers and then investigating the SCO behaviour.

Many solvent combinations that used methanol to dissolve the $\text{Fe}(\text{NCE})_2$ did not form the coordination networks, forming instead the methanol compounds **1** and **2**. However, experiments in which the 3,3'-bipyridine was dissolved in chloroform or bromoform produced crystals of stoichiometry $3 \cdot 2\text{CHCl}_3$, $3 \cdot 2\text{CHBr}_3$, $4 \cdot 2\text{CHCl}_3$ and $4 \cdot 2\text{CHBr}_3$, which were all shown by X-ray diffraction to contain parallel but non-planar

Table 2 Summary of crystallographic data for all structures

	1	2	3	3·2CHCl₃	3·2CHBr₃	4·2CHCl₃	4·2CHBr₃	4^a
Chemical formula	C ₂₄ H ₂₄ FeN ₆ O ₂ S ₂	C ₂₄ H ₂₄ FeN ₆ O ₂ Se ₂	C ₂₂ H ₁₆ FeN ₆ S ₂	C ₂₄ H ₁₈ FeN ₆ S ₂ Cl ₆	C ₂₄ H ₁₈ FeN ₆ S ₂ Br ₆	C ₂₄ H ₁₈ FeN ₆ Se ₂ Cl ₆	C ₂₄ H ₁₈ FeN ₆ Se ₂ Br ₆	C ₂₂ H ₁₆ FeN ₆ Se ₂
Formula Mass	548.46	642.26	484.38	723.11	989.87	816.92	1083.67	578.18
Crystal system	Triclinic	Triclinic	Monoclinic	Monoclinic	Monoclinic	Monoclinic	Monoclinic	Tetragonal
<i>a</i> /Å	8.2933(3)	8.6187(4)	8.6506(3)	17.053(8)	17.1155(3)	9.8578(13)	16.7183(10)	15.60597
<i>b</i> /Å	9.0510(3)	8.9469(4)	9.2253(3)	10.562(5)	10.4757(2)	12.8582(15)	11.0655(6)	15.60597
<i>c</i> /Å	9.0781(3)	9.1211(4)	14.1506(4)	18.440(9)	18.5942(3)	13.1284(16)	11.7733(7)	19.02474
α (°)	97.574(2)	94.987(2)	90.00	90.00	90.00	90.00	90.00	90.00
β (°)	96.833(2)	111.423(2)	94.430(2)	99.51(3)	98.9790(10)	96.601(6)	127.456(2)	90.00
γ (°)	111.473(2)	97.270(2)	90.00	90.00	90.00	90.00	90.00	90.00
Unit cell volume/Å ³	618.18(4)	642.69(5)	1125.91(6)	3276(3)	3293.03(10)	1653.0(4)	1728.95(17)	4633.405
<i>T</i> /K	200(2)	200(2)	200(2)	200(2)	100(2)	100(2)	200(2)	298(2)
Space group	<i>P</i> $\bar{1}$	<i>P</i> $\bar{1}$	<i>P</i> 2 ₁ / <i>n</i>	<i>C</i> 2/ <i>c</i>	<i>C</i> 2/ <i>c</i>	<i>P</i> 2 ₁ / <i>n</i>	<i>C</i> 2/ <i>m</i>	<i>I</i> 4/ <i>a</i>
<i>Z</i>	1	1	2	4	4	2	2	8
No. of reflections measured	12160	11180	11744	29832	13964	27672	8375	
No. of independent reflections	2835	2961	2598	4228	3797	3760	2719	
<i>R</i> _{int}	0.0145	0.0181	0.0216	0.0440	0.0217	0.0538	0.0272	
Final <i>R</i> ₁ values (<i>I</i> > 2σ(<i>I</i>))	0.0255	0.0175	0.0342	0.0632	0.0477	0.0392	0.0625	
Final <i>wR</i> (<i>F</i> ²) values (<i>I</i> > 2σ(<i>I</i>))	0.0751	0.0478	0.0870	0.1605	0.1188	0.0927	0.1580	
Final <i>R</i> ₁ values (all data)	0.0275	0.0191	0.0438	0.0938	0.0588	0.0593	0.0982	
Final <i>wR</i> (<i>F</i> ²) values (all data)	0.0768	0.0486	0.0950	0.1892	0.1260	0.1000	0.1799	

^a Data from indexing powder pattern.

two-dimensional grids formed from iron nodes and 3,3'-bipyridine edges, hosting solvent molecules between the layers. Selected bond lengths and angles are given in Table 3, and in all cases the iron-nitrogen distances are typical of high-spin iron(II) centres.

More interesting than individual bond-lengths and angles are the parameters of the networks, given in Table 3. In each case the (4,4) grid is rhomboid (Fig. 3a), with Fe–Fe distances along the edges that increase from 9.7 Å in the unsolvated case to 10.0–10.1 Å in the solvated cases. A much greater variation is seen in the corner angles, with the acute angle being smallest for unsolvated **3** (56.56°) and greatest for **4·2CHCl₃** (79.41°). In all cases, the iron atoms within a layer are all coplanar. There is considerable canting of the octahedral coordination sphere about the iron with respect to the plane of the grid, which means that the thio- or selenocyanate ligands do not protrude perpendicular to the plane; the deviation of the Fe–N bond from the

perpendicular is between 20 and 30°. The dihedral angle between the two rings of the bipyridine ligand varies from 180° in one case (an exact *anti* conformation, which is symmetry-imposed) to 139.37° in the unsolvated example.

The interplanar spacing is 7.118 Å in the unsolvated network **3**, but is expanded to between 8 and 10 Å in the solvated cases. In all cases, adjacent layers are offset so that an iron atom in one layer is above a rhomboidal space in the next.

Whilst the unsolvated thiocyanate-containing two-dimensional network **3** could be synthesised by reaction of its components in acetonitrile, this did not prove to be the case for the selenocyanate analogue **4**. We were unable to grow single crystals of **4** by diffusing its components together in acetonitrile, and simply mixing them yielded an orange powder whose XRPD pattern was not the same as generated by thermal decomposition of **2**. This pattern did, however, bear some similarities to that

Table 3 Selected bond lengths (Å) and angles (°) for the structures of **3** and **4**

	3	3·2CHCl₃	3·2CHBr₃	4·2CHCl₃	4·2CHBr₃
Fe–NCS	2.0849(16)	2.122(3)	2.124(3)	2.139(2)	2.130(5)
Fe–N _{bipy}	2.2502(15), 2.2744(16)	2.241(3), 2.250(3)	2.229(3), 2.240(3)	2.229(2), 2.265(2)	2.231(3)
Fe–N–CS	157.75(15)	162.1(2)	161.3(3)	161.8(2)	164.2(5)
Fe...Fe ^a	9.74	10.03	10.03	10.06	10.02
Fe...Fe...Fe ^b	56.6, 123.4	63.6, 116.4	62.9, 117.1	79.4, 100.6	67.0, 113.0
Spacing ^c	7.12	9.09	9.18	8.30	9.34
Dihedral ^d	139.4	160.0	161.9	157.9	180

^a The length of the sides of the rhombus defined by the iron atoms. ^b The angles at the corner of this rhombus. ^c The inter-layer spacing. ^d The dihedral angle between the two pyridyl rings of the 3,3'-bipyridine ligand.

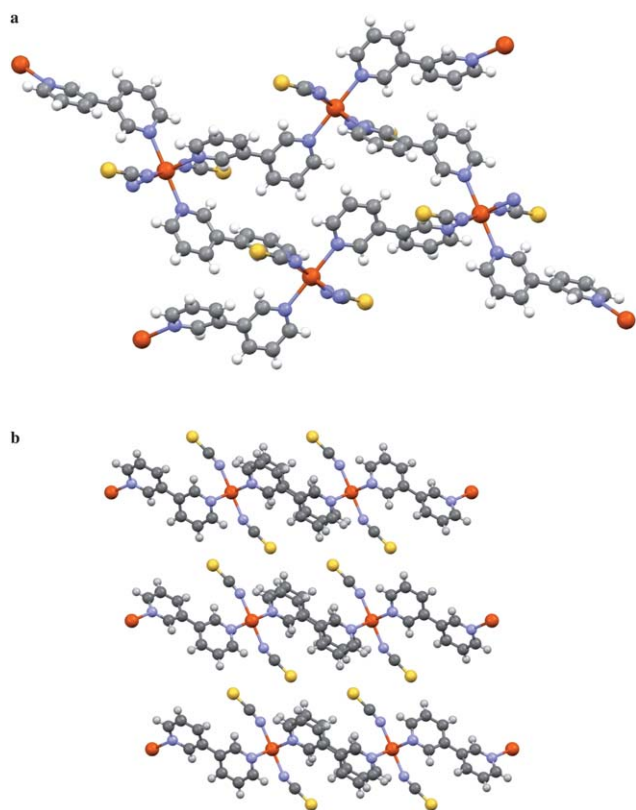


Fig. 3 (a) Part of the layered structure of **3**, showing how the iron atoms (orange) define a rhombus and the twisted nature of the 3,3'-bipyridine ligands. (b) Adjacent parallel layers in the structure of **3**, showing how the thiocyanate ligand is not perpendicular to the plane containing the iron atoms.

generated from the published structure of $\{\text{Ni}(\text{NCS})_2(3,3'\text{-bipy})_2\}$, and using this as a starting point we were able to index it in the same tetragonal space group $I4_1/a$, though with slightly longer cell axes ($a = b = 15.60$, $c = 19.02$ Å). Using the same fractional atom positions as for $\{\text{Ni}(\text{NCS})_2(3,3'\text{-bipy})_2\}$ (but

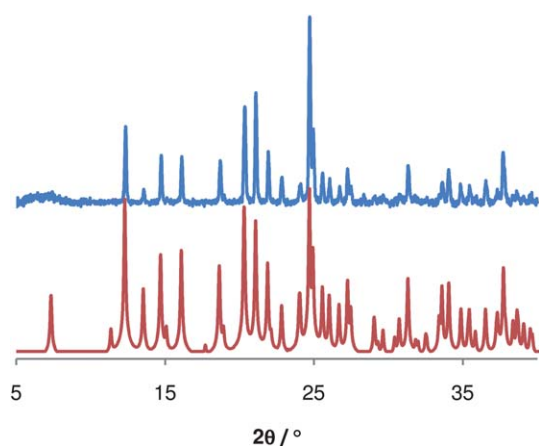


Fig. 4 Experimental powder pattern of **4** (blue) compared with a tetragonal model using the cell lengths $a = b = 15.60$, $c = 19.02$ Å and atom coordinates based on the published structure of $\{\text{Ni}(\text{NCS})_2(3,3'\text{-bipy})_2\}$ (with Fe and Se replacing Ni and S respectively).

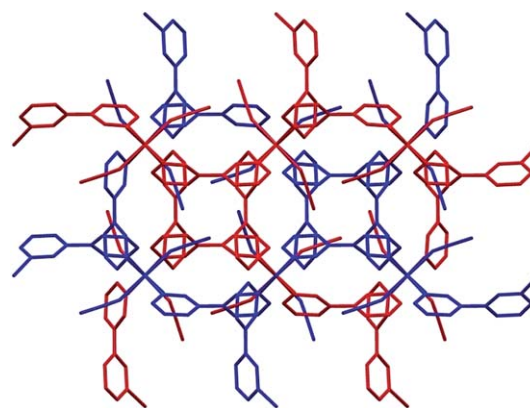


Fig. 5 The interpenetrated structure of **4**, with the two networks coloured blue and red.

replacing Ni and S with Fe and Se respectively) gave an excellent match to the experimental powder pattern (Fig. 4), so we conclude that the compound generated is indeed $\{\text{Fe}(\text{NCS})_2(3,3'\text{-bipy})_2\}$ **4**, but with an interpenetrating three-dimensional structure (Fig. 5) rather than the layered structure observed for its solvates. Details of this model are included in the ESI as a .cif file.

Conclusions

As we had hoped, the structures adopted by iron(II) thio- and selenocyanate systems with 3,3'-bipyridine mirrored those previously reported for other metals. We undertook this work due to our interest in spin-crossover systems, but all the crystal structures obtained contained the iron(II) centre in the high-spin state.

The 3,3'-bipyridine system presented above offers several parallels to the 4,4'-bipyridine system that we¹⁶ and others¹⁹ have studied. Thus, it is possible in both cases to form compounds with oxygen-donor molecules coordinated to the iron atom to give an FeN_4O_2 coordination sphere; herein the oxygen-donors are methanol, in $[\text{Fe}(\text{NCE})_2(3,3'\text{-bipy})_2(\text{MeOH})_2]$ **1** and **2**, whereas with 4,4'-bipyridine the compounds were the hydrates $\{[\text{Fe}(4,4'\text{-bipy})(\text{NCS})_2(\text{H}_2\text{O})_2] \cdot 4,4'\text{-bipy}\}$. In the latter case a 1D metal-containing polymer was formed containing hydrogen-bonded bipyridine molecules in the crystal lattice, in contrast to the monomeric methanol-containing compounds **1** and **2**, but the metal : ligand : solvent stoichiometry is the same in both cases—the difference is in how the ligands are arranged. There are previous reports of systems containing two monodentate bipyridine ligands coordinated to the same metal centre, but in these cases the ligand is 4,4'-bipyridine rather than the 3,3'-bipyridine of **1** and **2**.^{20,21}

Like **1** and **2**, $\{[\text{Fe}(4,4'\text{-bipy})(\text{NCS})_2(\text{H}_2\text{O})_2] \cdot 4,4'\text{-bipy}\}$ will undergo thermal decomposition, eliminating the oxygen-donor ligands and forming a layered 2-dimensional coordination polymer of composition $\{\text{Fe}(\text{bipy})_2(\text{NCE})_2\}$. Samples generated thermally are necessarily both powders and solvent-free, but use of the correct crystallisation conditions allows the isolation of multiple solvated structures which contain essentially the same 2D network acting as a host for guest solvent molecules, which lie

largely between the layers which have moved apart to accommodate them.¹⁶

A major difference from the 4,4'-bipyridine systems is in the structure of the unsolvated selenocyanate **4**, which adopts the interesting doubly-interpenetrated network reported for {Ni(NCS)₂(3,3'-bipy)₂}. No interpenetrated coordination networks have been reported for metal thio- or selenocyanate compounds with 4,4'-bipyridine, so it is possible that the greater flexibility offered by 3,3'-bipyridine allows this to occur. Unfortunately, we have been unable as yet to grow single crystals of this structure.

Experimental

3-Bromopyridine, FeSO₄·7H₂O, potassium thiocyanate and potassium selenocyanate were all purchased commercially and used as received.

Solvated crystals were grown by the following general method, performed in 35 ml screw-top vials: 3,3'-bipyridine (0.093 g, 0.6 mmol) was dissolved in 15 ml of CHX₃ and, depending upon the density, was layered either above or below a solution of FeSO₄·7H₂O (0.3 mmol) and KNCE (0.6 mmol) in 10 ml of the second solvent (either methanol or acetonitrile, as appropriate), which had previously been centrifuged to remove precipitated K₂SO₄. The lower solution was cooled by placing the vial in ice before layering, and a layer of the top solvent (containing no solutes) was placed between the layers before the top layer was added in order to prevent instant precipitation of powder. Generally this yielded crystals of the appropriate compound at the interface and microcrystalline powder at the bottom of the vial.

Crystallography

Single crystal X-ray data were collected on a Bruker APEX diffractometer using Mo-K α X-radiation, and corrected for absorption using empirical methods (SADABS) based upon symmetry-equivalent reflections combined with measurements at different azimuthal angles. Crystal structures were solved and refined against all F^2 values using the SHELXTL suite of programs.²² Non-hydrogen atoms were refined anisotropically and hydrogen atoms were placed in calculated positions refined using idealized geometries (riding model) and assigned fixed isotropic displacement parameters. Crystallographic details are contained in Table 2, and .cif files for all structures form part of the ESI. Within the crystal structure of **4**·2CHBr₃ there is some rotational disorder of both the solvent molecule and the pyridyl rings, which contributes to an R -factor of 6.25%. The structures of **3**·2CHCl₃ and **3**·2CHBr₃ also contain disordered solvent molecules.

Powder X-ray diffraction data were collected on a Bruker D8 advance powder diffractometer, operating at room temperature in reflection mode. The indexing of the powder pattern of **4** was performed using DASH.²³

Preparation of 3,3'-bipyridine

Pd(OAc)₂ (0.337 g, 1.5 mmol), [*n*-Bu₄N]Br (4.837 g, 15 mmol) and K₂CO₃ (4.140 g, 30 mmol) were dissolved in degassed DMF/H₂O (7 ml/3 ml) to give an orange solution. 3-Bromopyridine (2.95 ml, 30 mmol) was added and the solution heated to 115 °C

for 5 min causing a yellow solution to form. 2-Propanol (1.5 ml) was then added and the solution heated at 115 °C under N₂ for 3 days, resulting in a black suspension. Ethyl acetate (60 ml) was added and the solution filtered through Celite to remove K₂CO₃, which was further washed with more ethyl acetate (2 × 60 ml) to give an orange solution, which was dried over MgSO₄ and then evaporated to dryness to give an orange oil. The oil was dissolved in ethanol (50 ml) and 15% HCl (30 ml) added, before evaporating to dryness again to give an orange solid. The solid was suspended in EtOH/Et₂O (50 ml/50 ml) and filtered through a Buchner funnel to give the hydrochloride as a light orange solid. ¹H NMR (301 MHz, DMSO-*d*₆): δ (ppm) 6.50–7.50 (br s, 2H), 8.00 (dd, J = 8.07, 5.32 Hz, 2H), 8.77 (dt, J = 8.26, 1.84 Hz, 2H), 8.91 (dd, J = 5.32, 1.28 Hz, 2H), 9.32 (d, J = 2.20 Hz, 2H). The solid was suspended in CH₂Cl₂ (25 ml) and NEt₃ slowly added dropwise until no solid remained before being evaporated to dryness. Et₂O (4 × 15 ml) was added and the pale orange solution filtered through a pad of Alumina to give a pale yellow solution which was evaporated to dryness yielding a yellow oil, which solidified upon drying over P₂O₅ to give an off white solid (1.078 g, 46%). Anal. Calc. (Found) C₁₀H₈N₂·0.2H₂O C 75.16 (75.14), H 5.30 (5.32), N 17.53 (17.28). MS (EI, *m/z*): 156 (M). ¹H NMR (301 MHz, CDCl₃): δ (ppm) 7.42 (ddd, J = 7.94, 4.82, 0.83 Hz, 2H), 7.89 (dddd, J = 7.90, 2.39, 1.65, 0.76 Hz, 2H), 8.66 (dd, J = 4.86, 1.65 Hz, 2H), 8.85 (dd, J = 2.39, 0.73 Hz, 2H).

Preparation of [Fe(NCS)₂(3,3'-bipy)₂(MeOH)₂] **1**

3,3'-bipy (157 mg, 1.0 mmol) was dissolved in MeOH (5 ml) giving a pale yellow solution. In a separate flask FeSO₄ (139 mg, 0.5 mmol) and KNCS (98 mg, 1.0 mmol) were mixed in MeOH (5 ml) and then sonicated for 2 min before being centrifuged to remove K₂SO₄, giving an orange solution. The Fe(NCS)₂ solution was added dropwise to the 3,3'-bipy solution resulting in the precipitation of bright yellow microcrystals which were isolated by filtration with a Buchner funnel. 218 mg, 80%. Analysis Calc. for C₂₄H₂₄N₆O₂S₂Fe: C 52.56, H 4.41, N 15.32%. Found: C 52.76, H 4.09, N 15.31%.

Preparation of [Fe(NCSe)₂(3,3'-bipy)₂(MeOH)₂] **2**

3,3'-bipy (157 mg, 1.0 mmol) was dissolved in MeOH (5 ml) giving a pale yellow solution. In a separate flask FeSO₄ (139 mg, 0.5 mmol) and KNCSe (144 mg, 1.0 mmol) were mixed in MeOH (5 ml) and then sonicated for 2 min before being centrifuged to remove K₂SO₄ giving a yellow solution. The Fe(NCSe)₂ solution was added dropwise to the 3,3'-bipy solution, resulting in the precipitation of yellow microcrystals which were isolated by filtration with a Buchner funnel (244 mg, 76%). Analysis Calc. for C₂₄H₂₄N₆O₂Se₂Fe: C 44.88, H 3.77, N 13.09%. Found: C 44.65, H 3.82, N 12.78%.

Preparation of 2D [Fe(NCS)₂(3,3'-bipy)₂] **3**

3,3'-bipy (94 mg, 0.6 mmol) was dissolved in MeCN (8 ml) giving a colourless solution. In a separate flask FeSO₄ (84 mg, 0.3 mmol) and KNCS (59 mg, 0.6 mmol) were mixed in MeCN (10 ml) and then sonicated for 2 min before being centrifuged to remove K₂SO₄, giving a red solution. The Fe(NCS)₂ solution was added dropwise to the 3,3'-bipy solution, resulting in the

precipitation of a yellow powder which was isolated by filtration with a Buchner funnel (21 mg, 14%). Analysis Calc. for $C_{22}H_{16}N_6S_2Fe$: C 54.55, H 3.33, N 17.35%. Found: C 53.91, H 3.20, N 16.49%.

Preparation of 2D $[Fe(NCSe)_2(3,3'-bipy)_2]_4$

$[Fe(NCSe)_2(3,3'-bipy)_2(MeOH)_2]$ **2** (93 mg, 0.14 mmol) was placed in an oven under N_2 for 16 h giving a yellow-brown powder (83 mg, 99%). Analysis Calc. for $C_{22}H_{16}N_6Se_2Fe$: C 45.70, H 2.79, N 14.54%. Found: C 45.89, H 2.59, N 13.98%.

Preparation of 3D $[Fe(NCSe)_2(3,3'-bipy)_2]_4$

3,3'-bipy (94 mg, 0.6 mmol) was dissolved in MeCN (8 ml) giving a colourless solution. In a separate flask $FeSO_4$ (84 mg, 0.3 mmol) and $KNCSe$ (89 mg, 0.6 mmol) were mixed in MeCN (10 ml) and then sonicated for 2 min before being centrifuged to remove K_2SO_4 , giving a yellow solution. The $Fe(NCSe)_2$ solution was added dropwise to the 3,3'-bipy solution, resulting in the precipitation of a yellow-orange powder which was isolated by filtration through a Buchner funnel (14 mg, 8%). Analysis Calc. for $C_{22}H_{16}N_6Se_2Fe$: C 45.70, H 2.79, N 14.54%. Found: C 46.17, H 2.85, N 13.83%.

Acknowledgements

DJH wishes to thank the Royal Society of Chemistry for the award of a JWT Jones travelling fellowship, which enabled this work to be carried out.

References

- 1 K. Biradha, M. Sarkar and L. Rajput, *Chem. Commun.*, 2006, 4169.
- 2 E. C. Constable, D. Morris and S. Carr, *New J. Chem.*, 1998, **22**, 287.

- 3 G. F. Cavicholi, D. P. Martin, A. J. Ursini and R. L. LaDuca, *J. Mol. Struct.*, 2008, **881**, 107.
- 4 S. Lopez, M. Kahraman, M. Harmata and S. W. Keller, *Inorg. Chem.*, 1997, **36**, 6138.
- 5 M. Desciak, R. S. Rarig, J. Zubieta and R. L. LaDuca, *Acta Crystallogr., Sect. E: Struct. Rep. Online*, 2007, **63**, M435.
- 6 L. L. Johnston, A. J. Ursini, N. P. Oien, M. P. Desciak, R. S. Rarig, J. Zubieta and R. L. LaDuca, *Z. Anorg. Allg. Chem.*, 2008, **634**, 887.
- 7 R. L. LaDuca, C. Brodtkin, R. C. Finn and J. Zubieta, *Inorg. Chem. Commun.*, 2000, **3**, 248.
- 8 R. L. LaDuca, M. Desciak, M. Laskoski, R. S. Rarig and J. Zubieta, *J. Chem. Soc., Dalton Trans.*, 2000, 2255.
- 9 R. L. LaDuca, M. P. Desciak, R. S. Rarig and J. A. Zubieta, *Z. Anorg. Allg. Chem.*, 2006, **632**, 449.
- 10 R. S. Rarig, R. Lam, P. Y. Zavalij, J. K. Ngala, R. L. LaDuca, J. E. Greedan and J. Zubieta, *Inorg. Chem.*, 2002, **41**, 2124.
- 11 L. L. Johnston, A. J. Ursini, N. P. Oien, R. M. Supkowski and R. L. LaDuca, *Inorg. Chim. Acta*, 2007, **360**, 3619.
- 12 G. J. Halder and C. J. Kepert, *Aust. J. Chem.*, 2005, **58**, 311.
- 13 G. J. Halder, C. J. Kepert, B. Moubaraki, K. S. Murray and J. D. Cashion, *Science*, 2002, **298**, 1762.
- 14 N. Moliner, M. C. Muñoz, S. Létard, X. Solans, N. Menéndez, A. Goujon, F. Varret and J. A. Real, *Inorg. Chem.*, 2000, **39**, 5390.
- 15 J. A. Real, E. Andrés, M. C. Muñoz, M. Julve, T. Granier, A. Bousseksou and F. Varret, *Science*, 1995, **268**, 265.
- 16 C. J. Adams, J. A. Real and R. E. Waddington, *CrystEngComm*, 2010, **12**, 3547.
- 17 J. Hassan, V. Penalva, L. Lavenot, C. Gozzi and M. Lemaire, *Tetrahedron*, 1998, **54**, 13793.
- 18 H. Kanoh, A. Kondo, H. Noguchi, H. Kajiro, A. Tohdoh, Y. Hattori, W. C. Xu, M. Moue, T. Sugiura, K. Morita, H. Tanaka, T. Ohba and K. Kaneko, *J. Colloid Interface Sci.*, 2009, **334**, 1.
- 19 M. Wriedt, S. Sellmer and C. Näther, *Dalton Trans.*, 2009, 7975.
- 20 M. Felloni, A. J. Blake, N. R. Champness, P. Hubberstey, C. Wilson and M. Schröder, *J. Supramol. Chem.*, 2002, **2**, 163.
- 21 C. J. Adams, M. F. Haddow, M. Lusi and A. G. Orpen, *Proc. Natl. Acad. Sci. U. S. A.*, 2010, **107**, 16033.
- 22 G. M. Sheldrick, *Acta Crystallogr., Sect. A: Found. Crystallogr.*, 2008, **64**, 112.
- 23 W. I. F. David, K. Shankland, J. van de Streek, E. Pidcock, W. D. S. Motherwell and J. C. Cole, *J. Appl. Crystallogr.*, 2006, **39**, 910.